The glucocorticoid receptor agonistic modulators CpdX and CpdX-D3 do not generate the debilitating effects of synthetic glucocorticoids

Guoqiang Hua[a], Naimah Zein[a], Laetitia Paulen[a], and Pierre Chambon[a,b,c,1]

[a]Institut de Génétique et de Biologie Moléculaire et Cellulaire (IGBMC), CNRS UMR7104, INSERM U1258, 67404 Illkirch, France; [b]University of Strasbourg Institute for Advanced Study, 67404 Illkirch, France; and [c]Collège de France, 67404 Illkirch, France

Contributed by Pierre Chambon, May 23, 2019 (sent for review May 13, 2019; reviewed by Gerard Karsenty and Walter Wahli)

Seventy years after the discovery of their anti-inflammatory properties, glucocorticoids (GCs) remain the mainstay treatment for major allergic and inflammatory disorders, such as atopic dermatitis, asthma, rheumatoid arthritis, colitis, and conjunctivitis, among others. However, their long-term therapeutical administration is limited by major debilitating side effects, e.g., skin atrophy, osteoporosis, Addison-like adrenal insufficiency, fatty liver, and type 2 diabetes syndrome, as well as growth inhibition in children. These undesirable side effects are mostly related to GC-induced activation of both the direct transactivation and the direct transrepression functions of the GC receptor (GR), whereas the activation of its GC-induced indirect tethered transrepression function results in beneficial anti-inflammatory effects. We have reported in the accompanying paper that the nonsteroidal compound CpdX as well as its deuterated form CpdX-D3 selectively activate the GR indirect transrepression function and are as effective as synthetic GCs at repressing inflammations generated in several mouse models of major pathologies. We now demonstrate that these CpdX compounds are bona fide selective GC receptor agonistic modulators (SEGRAMs) as none of the known GC-induced debilitating side effects were observed in the mouse upon 3-mo CpdX treatments. We notably report that, unlike that of GCs, the administration of CpdX to ovariectomized (OVX) mice does not induce a fatty liver nor type 2 diabetes, which indicates that CpdX could be used in postmenopausal women as an efficient "harmless" GC substitute.

CpdX | glucocorticoid | selective glucocorticoid receptor agonistic modulators | undesirable side effects | type 2 diabetes

Despite several adverse effects, glucocorticoids (GCs) have been extensively used since the late 1940s of the past century to treat patients with allergic and inflammatory disorders (1). GC functions are transduced by a single receptor, the GR, which, upon GC binding, exerts one of its three main functions by regulating the transcription of target genes through: (*i*) (+) GC-responsive element (GRE)-mediated direct transactivation (2), (*ii*) IR nGRE-mediated direct transrepression (3–5), and (*iii*) tethered transrepression of transcriptional activators, such as NFκB, AP1, and STAT3 (5–8). The GC-associated beneficial anti-inflammatory activity of the GR has been mostly ascribed to tethered transrepression, whereas GC-associated undesirable debilitating side effects appear to result from both direct transactivation (1) and direct transrepression (3, 4). Consequently, selective GC receptor agonistic modulators (SEGRAMs) that would preferentially induce tethered transrepression, whereas being devoid of both direct transactivation and direct transrepression activities, have been actively sought during the past two decades. Several synthetic nonsteroidal putative SEGRAMs, such as mapracorat/ZK 245186 (9, 10), CpdA (11), ZK 216348 (12), AL-438 (13), Org 214007–0 (14), and AZD9567 (15), among others, have been identified and claimed to exhibit some GC-like anti-inflammatory activities, whereas exhibiting less GC-induced undesirable effects than synthetic GCs.

We previously identified a possible SEGRAM candidate that we named CpdX, which selectively induces the GR indirect transrepression activity (8) and are now reporting in the accompanying paper that CpdX and its racemic deuterated form CpdX-D3 as well as their respective enantiomers selectively and efficiently induce the anti-inflammatory and antiallergic activities of synthetic GCs [e.g., dexamethasone (Dex)] in several mouse inflammatory models (16). We report here that, in marked contrast to a treatment with a synthetic GC (e.g., Dex), a 3-mo treatment with CpdX, CpdX-D3, or one of their enantiomers does not induce any of the "classical" long-term GC-induced undesirable side effects.

Results

Unlike Dex, a Topical Treatment of Mouse Skin with CpdX, CpdX-D3, or One of Their Enantiomers Does Not Induce a Skin Epidermal Atrophy. Skin atrophy is a severe limitation to topical GC treatments (17). To investigate whether, similar to Dex, a CpdX topical administration could induce a skin atrophy, ethanol (vehicle), Dex, CpdX, its deuterated form CpdX-D3, or one of their enantiomers CpdX(eA), CpdX(eB), CpdX-D3(eA), or CpdX-D3(eB) were topically applied daily for 8 d to the shaved dorsal skin of Balb/C mice. Mice were killed, and histological analyses were performed. Hematoxylin–eosin (H–E) staining revealed that a Dex application severely induces an epidermal atrophy (down to a single-cell

Significance

Despite their beneficial anti-inflammatory and antiallergic effects, the clinical long-term administration of synthetic glucocorticoids (GCs) is limited by a number of severe side effects. During the last 20 y, several so-called selective GC receptor agonistic modulators (SEGRAMs) have been reported and claimed to be less debilitating than GCs while keeping their long-term beneficial anti-inflammatory properties. However, none of these possible SEGRAMs have been fully tested for undesirable detrimental effects that may occur upon long-term therapy in vivo. We now report that the anti-inflammatory compounds CpdX and CpdX-D3 as well as their enantiomers are bona fide "harmless" SEGRAMs as, upon 3-mo-long administration to mice, none of the known GC-induced debilitating side effects were observed.

Author contributions: G.H., N.Z., and P.C. designed research; G.H., N.Z., and L.P. performed research; G.H., N.Z., L.P., and P.C. analyzed data; and G.H. and P.C. wrote the paper.

Reviewers: G.K., Columbia University Medical Center; and W.W., Nanyang Technological University Singapore.

Conflict of interest statement: An International patent application was filed on 23 October 2018 under the number PCT/EP2018/079049.

[1]To whom correspondence may be addressed. Email: chambon@igbmc.fr.

This article contains supporting information online at www.pnas.org/lookup/suppl/doi:10.1073/pnas.1908264116/-/DCSupplemental.

Published online June 20, 2019.

thickness) in marked contrast to an application of CpdX, its deuterated form CpdX-D3, or of any of their enantiomers (Fig. 1*A*). Morphometric analyses showed that the epidermal thickness decreases by 70% upon a Dex treatment, whereas it was not decreased upon CpdX, CpdX(eA), CpdX(eB), CpdX-D3, CpdX-D3(eA), or CpdX-D3(eB) administration (Fig. 1*B*). Note that similar data were obtained upon 3-wk topical treatments and that a 3-mo s.c. administration of either Dex or CpdX did not induce a skin atrophy.

It is known that a "genetic" loss of the kindlin-1 protein results in an epidermal skin atrophy (18), whereas the loss of the Redd1 protein prevents a GC-induced skin atrophy (19, 20). RNA transcripts were extracted from dorsal skin samples, and transcripts of kindlin-1 and REDD1 genes were analyzed by q-RT-PCR. The transcription of the kindlin-1 gene, which contains putative nGREs located at positions −9884 bp (CTCCcaGGAGg), −6414 bp (CTCCTGAGa), and −5964 bp (CTCCtTGAG) from the transcription start site, was strongly decreased by a Dex topical treatment but not by CpdX, CpdX(eA), CpdX(eB), CpdX-D3, CpdX-D3(eA), or CpdX-D3(eB) treatments (Fig. 1 *C*, *Left*). Conversely, the transcription of the REDD1 gene that contains a +GRE (19) was significantly increased upon administration of Dex but not of CpdX, CpdX(eA), CpdX(eB), CpdX-D3, CpdX-D3(eA), or CpdX-D3(eB) (Fig. 1 *C*, *Right*). Similar data were obtained upon 3-wk topical treatments. Taken altogether, the above data demonstrate that our CpdX compounds behave as bona fide SEGRAMs in vivo.

It has been reported that the synthetic nonsteroidal ligand mapracorat (also known as ZK245186 or BOL-303242-X) could be a promising anti-inflammatory drug for skin diseases (10, 21). However, we found that a short 8-d topical treatment with mapracorat induced a significant atrophy of dorsal skin epidermis (Fig. 1*A*), whereas the transcription of the kindlin-1 gene was actually decreased by mapracorat, whereas that of the REDD1 gene was increased (Fig. 1*C*). Our present results demonstrate that, in marked contrast to a Dex or a mapracorat topical treatment, a topical skin treatment with CpdX, its deuterated form CpdX-D3, or with one of their enantiomers [CpdX(eA), CpdX(eB), CpdX-D3(eA), or CpdX-D3(eB)] did not result in an epidermal skin atrophy, indicating that CpdX and CpdX-D3 as well as their enantiomers can be "safely" used in skin treatments.

Unlike Dex, a 3-Mo Mouse Treatment with CpdX or CpdX-D3 and with One of Their Enantiomers Does Not Affect Bone Formation. Osteoporosis is a common undesirable side effect of long-term

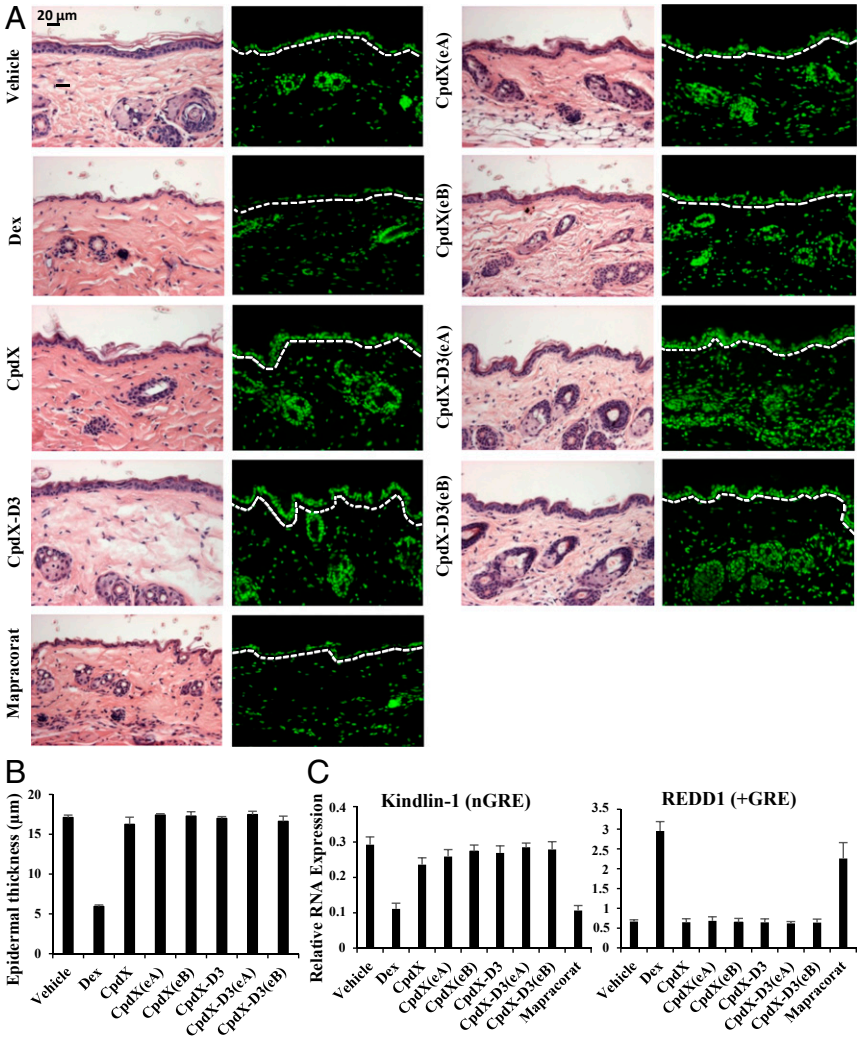

Fig. 1. Unlike Dex, a topical treatment of mouse skin with CpdX, CpdX-D3, or one of their enantiomers does not induce a skin epidermal atrophy. (*A*) H–E staining (*Left*) and DAPI staining for nuclei (*Right*) of sections of mouse ears treated as indicated (Scale bar represents 20 μm). (*B*) Morphometric analysis of the epidermal thickness (in μm) from H–E stained ear sections as under (*A*). (*C*) Q-RT-PCR for transcripts of kindlin-1 and REDD1 genes in mouse ears treated as indicated. Data are represented as mean ± SEM of, at least, three independent experiments with, at least, three mice per treatment.

clinical treatments with GCs (22). To study whether a long-term CpdX treatment could induce osteoporosis, 8-wk-old B6 male mice were subjected daily for 3 mo to a s.c. injection of vehicle (NaCl 0.9%), Dex, CpdX, CpdX(eA), CpdX(eB), CpdX-D3, CpdX-D3(eA), or CpdX-D3(eB) (1 mg/kg body weight, diluted in NaCl 0.9%). One femur and the ipsilateral tibia were dissected from each mouse and preserved in 70% ethanol for further microcomputed tomography (micro-CT) bone microstructure analysis. Following a 3-mo Dex treatment, osteoporosislike phenotypes were observed in the tibia cortical bone: The bone volume was significantly decreased compared with the total volume (Fig. 2*A*), the cortical thickness was drastically decreased (Fig. 2*B*), whereas the bone area but not the marrow area was also reduced (Fig. 2 *C* and *D*). Surprisingly, but in agreement with a previous report (23), a Dex treatment increased

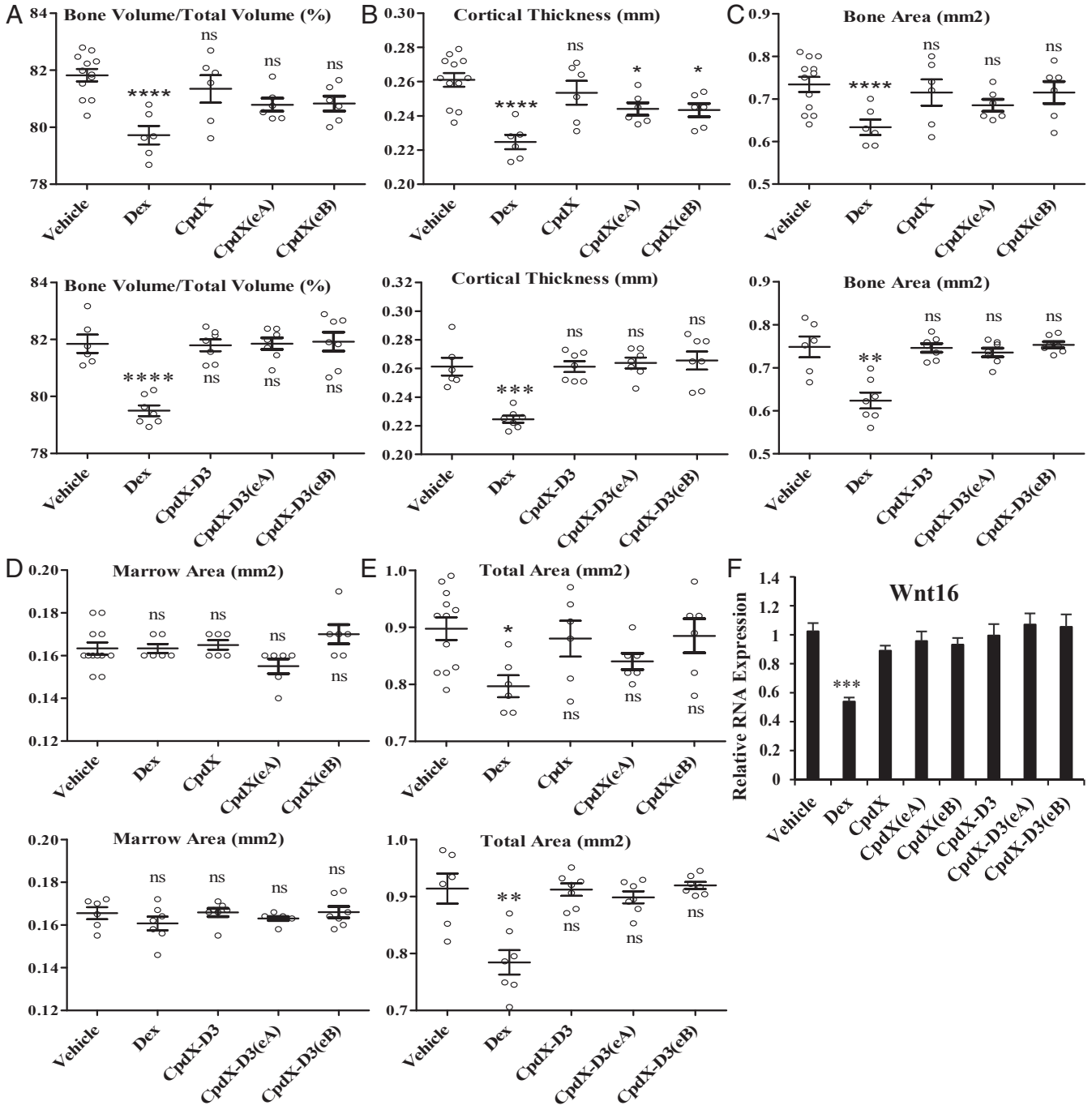

Fig. 2. Unlike Dex, a 3-mo mouse treatment with CpdX, CpdX-D3, or their enantiomers does not affect bone formation. Five cortical bone parameters were measured by micro-CT: (*A*) bone volume/total volume (%); (*B*) cortical thickness (mm); (*C*) bone area (mm^2), (*D*) marrow area (mm^2) and (*E*) total area (mm^2); the data correspond to the mean ± SEM for, at least, six mice per treatment. The statistical significance compared with vehicle treatment was calculated through a one-way ANOVA test followed by Dunnett's multiple comparison test (*) $P < 0.05$; (**) $P < 0.01$; (***) $P < 0.001$; (****) $P < 0.0001$; (ns): not significant. (*F*) Q-RT-PCR for transcripts of the WNT16 gene in tibia from mice treated as indicated. Data are represented as mean ± SEM with, at least, six mice per treatment. The statistical significance was calculated by Student *t* test; (***) $P < 0.001$.

the mouse trabecular bone volume due to a higher number of trabeculae and to a decrease in the trabecular spacing, whereas the trabecular thickness was not affected. Importantly, in marked contrast to a Dex treatment, a 3-mo administration of CpdX or CpdX-D3 as well as of one of their enantiomers CpdX(eA), CpdX(eB), CpdX-D3(eA), or CpdX-D3(eB) did not affect the formation of cortical and trabecular bones (Fig. 2 *A*–*E*).

A decrease in the expression of the WNT16 gene is known to affect the bone mineral density, the cortical bone thickness, and the bone strength and to increase the risk of osteoporotic fractures (24). Q-RT-PCR analyses of transcripts of the WNT16 gene, which contains several putative nGREs at positions −5225 bp (CTCCcgGGAGc), −4732 bp (CTCCtgGGCGa), −3839 bp (CTCCaGGATg), and −65 bp (CTCCaGGCGc), demonstrated that the transcription of the WNT16 gene was decreased by 50% in mouse tibia samples upon a Dex treatment but not upon CpdX, CpdX(eA), CpdX(eB), CpdX-D3, CpdX-D3(eA), or CpdX-D3(eB) administration (Fig. 2*F*).

Taken altogether, the above data indicate that, unlike synthetic GCs (e.g., Dex), CpdX and CpdX-D3 as well as any of their enantiomers [CpdX(eA), CpdX(eB), CpdX-D3(eA), or CpdX-D3(eB)] could be safely used for clinical treatments of inflammatory diseases as they do not affect bone formation.

Unlike Dex, a 3-Mo Treatment with CpdX, CpdX-D3, or Any of Their Enantiomers Does Not Lead to a Loss of Body Weight, a Change in Body Composition, nor Undesirable Tissue-Specific "Toxic" Side Effects. A dual-energy X-ray absorptiometry machine (25) was used to determine both the mouse lean and the mouse fat masses after 3-mo treatments (as described above). All mice treated with vehicle, CpdX, CpdX-D3, or any of their enantiomers, exhibited similar increases in body weight (Fig. 3*A*) as well as commensurate increases in fat mass (Fig. 3*B*) and lean percentage (Fig. 3*C*). In contrast, mice treated with Dex exhibited a net loss in total body weight (Fig. 3*A*) together with a disproportional increase in fat (Fig. 3*B*) and a decrease in lean mass (Fig. 3*C*).

GCs are well known to induce a drastic thymus apoptosis (26). Accordingly, after a 3-mo treatment, no thymus was found in 16 out of 19 Dex-treated mice. In marked contrast, treatments with CpdX, its deuterated form CpdX-D3, or their enantiomers [CpdX(eA), CpdX(eB), CpdX-D3(eA), or CpdX-D3(eB)] did not result in any significant thymus apoptosis (Fig. 3*D*). The spleen weight was decreased by more than 50% in Dex-treated mice but not in CpdX-, CpdX(eA)-, CpdX(eB)-, CpdX-D3-, CpdX-D3(eA)-, or CpdX-D3(eB)-treated mice (Fig. 3*E*). A weak but significant loss of kidney weight was also selectively observed in mice treated with Dex (Fig. 3*F*). Interestingly, the weight of the adrenal gland in which corticosterone synthesis takes place was decreased by a Dex treatment but significantly increased by CpdX, CpdX(eA), CpdX(eB), CpdX-D3, CpdX-D3(eA), or CpdX-D3(eB) treatments (Fig. 3*G*).

A Long-Term Daily s.c. Injection of Dex Inhibits Corticosterone Synthesis Which, in Marked Contrast, Is Increased upon a Similar Treatment with CpdX, CpdX(eA), CpdX(eB), CpdX-D3, CpdX-D3(eA), or CpdX-D3(eB). Corticosterone is known to be synthesized in the fasciculata zone of the cortex layer of the adrenal gland. Histological sections showed that, upon a 3-mo treatment with Dex, the thickness of the

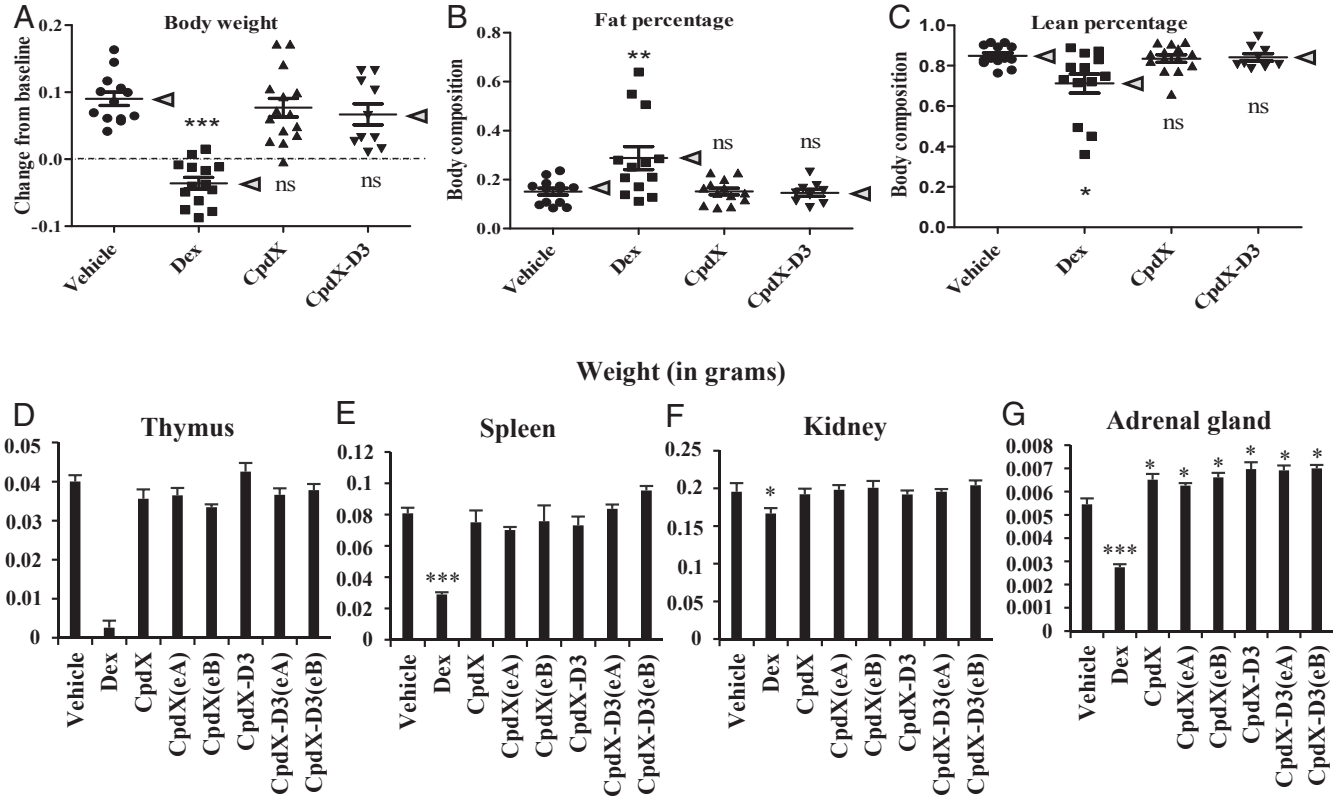

Fig. 3. Unlike Dex, a 3-mo treatment with CpdX, CpdX-D3, or any of their enantiomers does not lead to a loss of body weight, a change in body composition, or undesirable tissue-specific toxic side effects. (*A*) Change in body weight after a 3-mo treatment. (*B*) Fat percentage and (*C*) lean mass percentage for mice treated for 3 mo. The data correspond to the mean (as pointed out by arrow heads) ± SEM for, at least, nine mice per treatment. The statistical significance was calculated through the Krustal–Walis test followed by Dunn's multiple comparison test; (*) $P < 0.05$; (**) $P < 0.01$; (***) $P < 0.001$; (ns): not significant. Weight (in grams) of thymus (*D*), spleen (*E*), kidney (*F*), and adrenal gland (*G*) in mice treated for 3 mo as indicated. Data are represented as mean ± SEM for, at least, nine mice per treatment. The statistical significance of the data, compared with vehicle treatment was calculated by Student *t* test; (*) $P < 0.05$; (***) $P < 0.001$.

cortex layers (see double-headed arrows in the upper panels), most notably the fasciculata zone (see bold double-headed arrows in the lower panels), were drastically decreased (Fig. 4*A*), whereas, in marked contrast, they were increased upon the administration of CpdX, of its deuterated form CpdX-D3, or of one of their enantiomers CpdX(eA), CpdX(eB), CpdX-D3(eA), or CpdX-D3(eB) (Fig. 4*A*). Transcriptional analyses from mouse adrenal gland samples demonstrated that the transcripts of the Cyp11a, Cyp11b1, and HSD3β genes, which are all involved in corticosterone biosynthesis (27), were significantly repressed by Dex treatment [due to

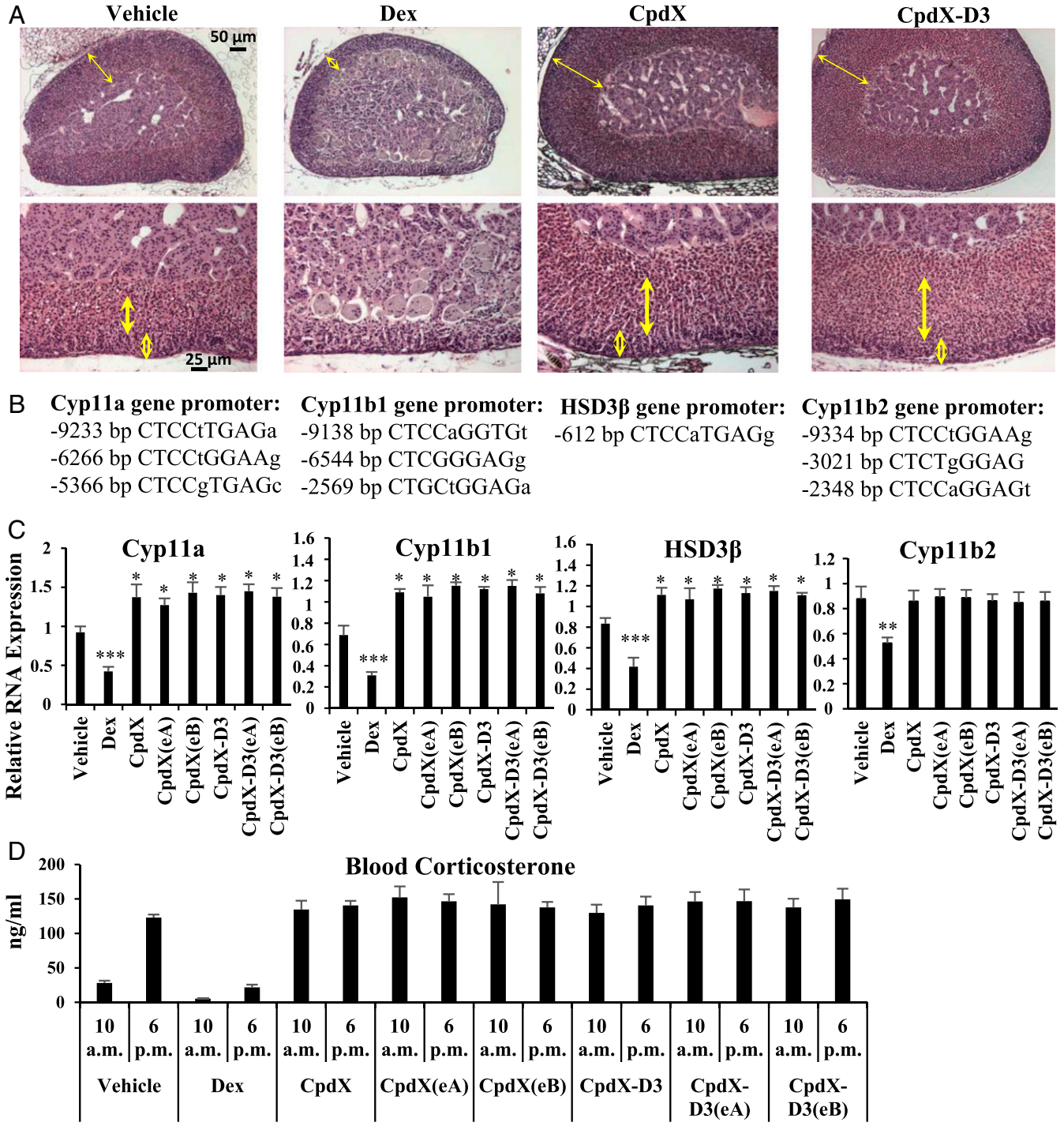

Fig. 4. A long-term daily s.c. injection of Dex inhibits corticosterone synthesis which, in marked contrast, is increased upon a similar treatment with CpdX, CpdX(eA), CpdX(eB), CpdX-D3, CpdX-D3(eA), or CpdX-D3(eB). (*A*) H–E staining of adrenal gland sections. The cortex layer of the adrenal gland is indicated in *Left* by double-headed thin arrows, whereas the fasciculata and the glomerulosa zones of the cortex are indicated by long bold double-headed arrows and small empty double-headed arrows in *Right*, respectively (Scale bar represents 50 and 25 μm, respectively). (*B*) Locations of nGREs present in the promoter regions of Cyp11a, Cyp11b, HSD3β, and Cyp11b2 genes. (*C*) Q-RT-PCR for transcripts of Cyp11a, Cyp11b1, HSD3β, and Cyp11b2 genes in adrenal glands of mice treated for 3 mo as indicated. Data are represented as mean ± SEM for, at least, nine mice per treatment. The statistical significance of the data compared with vehicle treatment was calculated by Student *t* test; (*) $P < 0.05$; (**) $P < 0.01$; (***) $P < 0.001$. (*D*) Plasmatic corticosterone levels at 10 AM and 6 PM in mice treated for 3 mo as indicated. Data are represented as mean ± SEM with, at least, nine mice per treatment.

the presence of nGREs in these genes (Fig. 4*B*)], whereas being derepressed upon treatment with CpdX, CpdX(eA), CpdX(eB), CpdX-D3, CpdX-D3(eA), or CpdX-D3(eB), which cannot induce the binding of GR to nGREs (Fig. 4*C*).

Compared with control vehicle-treated mice, Dex-treated mice exhibited much lower corticosterone levels in plasma at both 10 AM and 6 PM, whereas, in marked contrast, CpdX-, CpdX(eA)-, CpdX(eB)-, CpdX-D3-, CpdX-D3(eA)-, and CpdX-D3(eB)-treated mice showed a much higher corticosterone level at 10 AM (Fig. 4*D*), indicating that the circadian control of corticosterone synthesis was lost in CpdX-treated mice.

Interestingly, transcriptional analyses from mouse adrenal gland samples also showed that the transcription of the Cyp11b2 gene which is involved in aldosterone biosynthesis was inhibited by Dex treatment but not by CpdX, CpdX(eA), CpdX(eB), CpdX-D3, CpdX-D3(eA), or CpdX-D3(eB) treatments (Fig. 4*C*). Note, in this respect, that the Cyp11b2 gene also contains a nGRE motif (Fig. 4*B*). In agreement with these data, histological analyses revealed that the size of the glomerulosa zone (the outermost zone of the cortex layer, see the small empty double-headed arrows in the lower panels of Fig. 4*A*), which produces aldosterone, was drastically decreased by Dex treatment but not by CpdX, CpdX(eA), CpdX(eB), CpdX-D3, CpdX-D3(eA), or CpdX-D3(eB) (Fig. 4*A*).

Unlike Dex, a 3-Mo Treatment with CpdX, CpdX-D3, or Any of Their Enantiomers Does Not Induce Type 2 Diabetes Syndrome nor a Fatty Liver. Hyperglycemia is a common undesirable side effect of a long-term GC administration (28). Upon a 3-mo treatment, the overnight fasting blood glucose level was significantly higher in Dex-treated mice than in mice treated with saline (vehicle), CpdX, CpdX(eA), CpdX(eB), CpdX-D3, CpdX-D3(eA), or CpdX-D3(eB) (Fig. 5*A*). An IPGTT showed that, upon glucose injection to Dex-treated mice, the blood glucose level was significantly higher during a 2-h period, whereas no significant differences among these levels was observed in the Control, CpdX-, CpdX(eA)-, CpdX(eB)-, CpdX-D3-, CpdX-D3(eA)-, or CpdX-D3(eB)-treated mice (Fig. 5*B*). Taken altogether these data indicate that, unlike a Dex administration, a treatment with CpdX, CpdX(eA), CpdX(eB), CpdX-D3, CpdX-D3(eA), or CpdX-D3(eB) does not induce hyperglycemia.

A long-term treatment with GCs is known to result in an insulin resistance (29). Upon a 3-mo GC treatment, Dex-treated mice exhibited hyperinsulinemia, in marked contrast to mice treated with saline (vehicle), CpdX, CpdX(eA), CpdX(eB), CpdX-D3, CpdX-D3(eA), or CpdX-D3(eB) (Fig. 5*C*). This hyperinsulinemia, taken together with an IPITT, which revealed a significant impaired response to insulin (Fig. 5*D*), indicates the occurrence of an insulin resistance in Dex-treated mice (29). In keeping with this resistance, western-blot analyses (Fig. 5*E*) of liver extracts revealed that, in Dex-treated mice, the phosphorylated insulin receptor substrate 1 (p-IRS1 S318) was 40–50% lower than in CpdX- or CpdX-D3-treated mice. As expected, the phosphorylation of the insulin-stimulated protein kinase B (p-AKT S473) was also decreased by 50–60% in Dex-treated mice compared with CpdX- or CpdX-D3-treated mice (Fig. 5*E*) (30). Taking these data altogether, we conclude that, unlike Dex, treatments with CpdX, its deuterated form CpdX-D3, or any of their enantiomers [CpdX(eA), CpdX(eB), CpdX-D3(eA), and CpdX-D3(eB)], do not induce hyperglycemia and insulin resistance that are characteristic of type 2 diabetic syndrome.

Interestingly, 5% red oil stained frozen sections of liver samples harvested at the end of these 3-mo treatments revealed a lipid deposition in livers from mice subjected to a daily s.c. administration of Dex but not in livers from mice treated with vehicle, CpdX, CpdX-D3, or their respective enantiomers (Fig. 5*F*). In keeping with these lipid depositions, an increase in RNA transcripts of the FASN and SCD1 genes that are both critically involved in liver lipogenesis (31) was observed in the liver of Dex-treated but not in vehicle, CpdX, CpdX(eA), CpdX(eB), CpdX-D3, CpdX-D3(eA), or CpdX-D3(eB)-treated mice (Fig. 5*G*).

Hypercholesterolemia is associated with nonalcoholic fatty liver diseases (32), and cholesterol is known to be converted in the liver into bile acids (33). Accordingly, Dex-treated but not CpdX-, CpdX(eA)-, CpdX(eB)-, CpdX-D3-, CpdX-D3(eA)-, or CpdX-D3(eB)-treated mice exhibited a significant increase in blood cholesterol and bile acid levels (Fig. 5*H*).

Taken altogether, the above data demonstrate that a 3-mo administration of CpdX, its deuterated derivative CpdX-D3, or any of their respective enantiomers [CpdX(eA), CpdX(eB), CpdX-D3(eA), and CpdX-D3(eB)] does not induce type 2 diabetes syndrome nor a fatty liver disease, in marked contrast with a similar treatment with the synthetic GC Dex.

In Marked Contrast with Dex, a 1-Mo Treatment with CpdX Decreases the Plasmatic Glucose Level and Liver Lipid Deposition in OVX Mice. It has been reported that an estrogen deficiency can lead to hyperglycemia and a fatty liver lipid deposition in the liver of postmenopausal women (34) as well as in the livers of 4-mo-old mice that were OVX at the age of 4 wk (35). It is also known that a long-term treatment with GCs (Dex) can aggravate these metabolic and hepatic syndromes (35). To investigate whether a CpdX administration could possibly prevent the occurrence of such syndromes in postmenopausal women, bilaterally OVX mice were taken as surgical models for menopause. Three months postsurgery, OVX mice were i.p. injected daily for a month with Dex, CpdX, or saline. Increases in fasting plasmatic glucose levels (Fig. 6*A*) and in liver lipid deposition (Fig. 6*B*) were observed in OVX mice (compared with sham-operated control mice). Most notably, these increases were significantly higher in Dex-treated OVX mice (Fig. 6 *A* and *B*). Interestingly, the plasmatic glucose level returned to normality, whereas the liver lipid deposition was drastically reduced upon a 1-mo CpdX treatment and comparable to that of untreated sham-operated mice (Fig. 6 *A* and *B*). Accordingly, RNA transcript analyses revealed an increase in the expression of the FASN and SCD1 genes in OVX mice, compared with the control mice. Interestingly, a Dex treatment of OVX mice markedly increased the expression of these two genes, whereas a CpdX treatment significantly decreased their expression to those of sham-operated control mice (Fig. 6*C*).

Taken together, these results reveal that both the elevated blood glucose level and the increase in liver lipid deposition, which occur within 3-mo postovariectomy, are prevented by a CpdX administration during the last month. Most interestingly, a similar treatment with Dex aggravates these metabolic and hepatic syndromes. These data strongly suggest that the administration of CpdX to postmenopausal women could be a much better and safer anti-inflammatory treatment than "traditional" GC treatments and, furthermore, could be used to cure estrogen deficiency-induced metabolic and hepatic disorders (i.e., fatty liver) in postmenopausal women.

As CpdX was initially described in 1998 among a series of synthetic nonsteroidal gestagen compounds (36), we investigated whether it may exhibit any estrogenic and/or progesterone activity. To this end, Cos-1 cells were transfected with either an estrogen or a progesterone receptor expression vector and a cognate luciferase (Luc) reporter that contains either a 17-mer estrogen or a two times repeated progesterone binding element (pGL3-17mer-ERE or pLuc-TK-2xPRE). Twenty-four h post-transfection, cells were treated with estradiol, progesterone, Dex, CpdX, or CpdX-D3 for 6 h. Luc assays showed that estradiol and progesterone did induce Luc activity, whereas Dex, CpdX, or CpdX-D3 could not (Fig. 6 *D* and *E*). In addition, this estradiol-induced Luc activity was inhibited by tamoxifen, a well-known competitive inhibitor of estrogen activity, thus confirming that the estrogen receptor-specific Luc

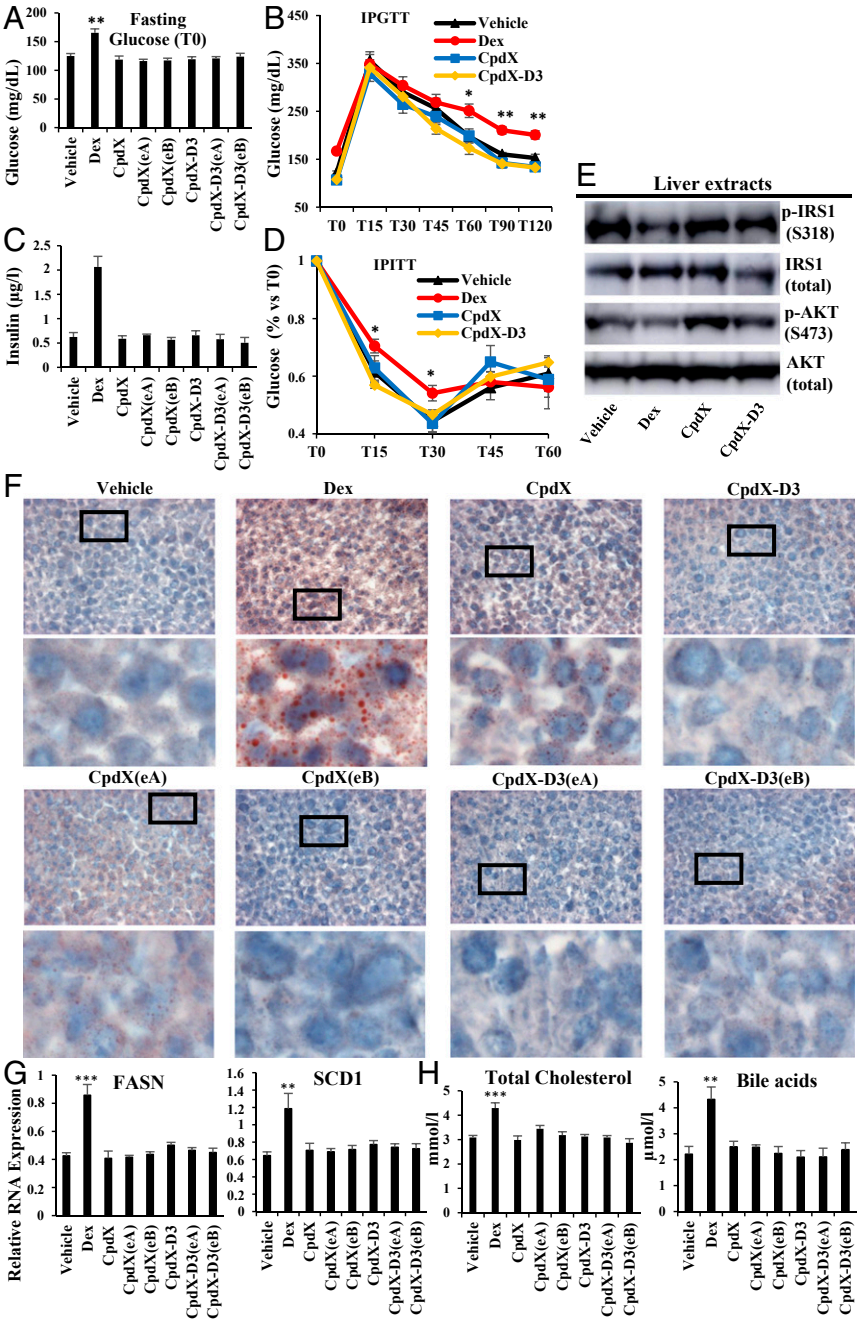

Fig. 5. Unlike Dex, a 3-mo treatment with CpdX, CpdX-D3, or any of their enantiomers does not induce type 2 diabetes syndrome nor a fatty liver. (*A*) Plasmatic glucose levels (after an overnight 14-h fasting) from mice treated for 3 mo as indicated. Data are represented as mean ± SEM for, at least, nine mice per treatment as indicated. The statistical significance of the data, compared with vehicle treatment, was calculated by Student *t* test; (**) $P < 0.01$. (*B*) Two-h i.p. glucose tolerance test (IPGTT) after a glucose i.p. injection (2 mg/kg body weight). Data are represented as mean ± SEM for, at least, six mice per treatment as indicated. The statistical significance of the data, compared with vehicle treatment, was calculated by Student *t* test; (*) $P < 0.05$; (**) $P < 0.01$. (*C*) Blood insulin levels (µg/L) at 10 AM in mice treated for 3 mo as indicated. Data are represented as mean ± SEM for, at least, nine mice per treatment. (*D*) One-h i.p. insulin tolerance test (IPITT) after an i.p. injection of 0.75 U Insulin/kg body weight. Data are represented as mean ± SEM with, at least, six mice per treatment. The statistical significance compared with vehicle treatment was calculated by Student *t* test, (*) $P < 0.01$. (*E*) Western blot analyses of liver samples of mice treated for 3 mo as indicated for phosphoinsulin receptor substrate-1 phosphorylated at serine 318 (p-IRS1 S318), pan-insulin receptor substrate-1 (IRS total), phosphoprotein kinase B phosphorylated at serine 473 (p-AKT S473), and pan-protein kinase B (AKT total) proteins. (*F*) A 5% red oil staining of frozen liver sections from mice treated for 3 mo as indicated. In each case, the *Lower* is an enlargement of the region located within the square as indicated in the *Upper*. (*G*) Q-RT-PCR for transcripts of fatty acid synthase (FASN) and stearoyl-CoA desaturase 1 (SCD1) genes in livers of mice treated for 3 mo as indicated. The data correspond to the mean ± SEM for, at least, nine mice per treatment. The statistical significance was calculated by Student *t* test; (**) $P < 0.01$; (***) $P < 0.001$. (*H*) Levels of total cholesterol (mmol/L) and bile acids (µmol/L) in blood collected at 10 AM from mice treated for 3 mo as indicated. Data are represented as mean ± SEM for, at least, nine mice per treatment.

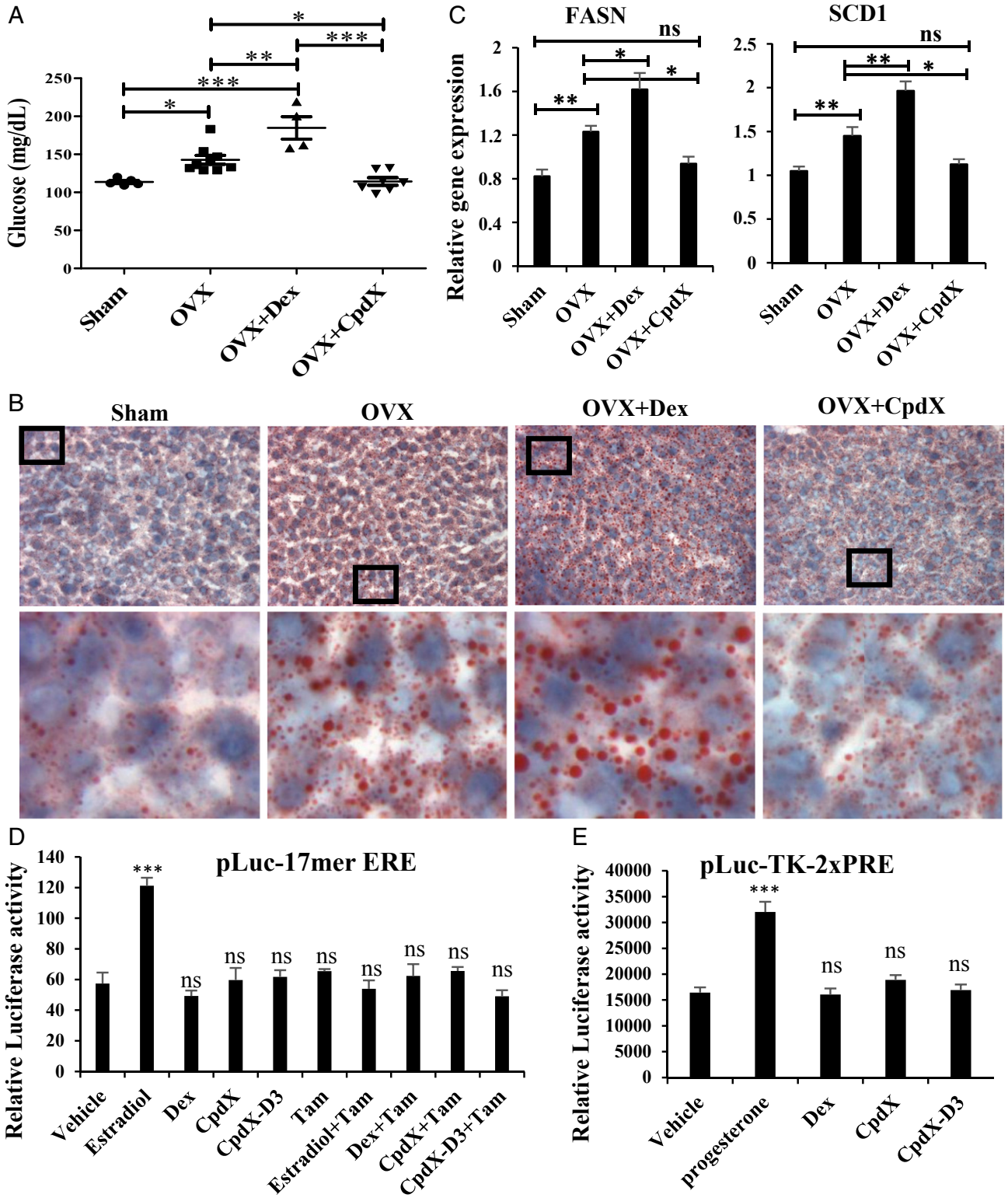

Fig. 6. In marked contrast with Dex, a 1-mo treatment with CpdX decreases the plasmatic glucose level and liver lipid deposition in OVX mice. (*A*) Plasmatic glucose levels after an overnight 14-h fasting of either sham or OVX mice treated for 1 mo as indicated. The statistical significance was calculated through a one-way ANOVA test followed by Tukey's multiple comparison test (*) $P < 0.05$; (**) $P < 0.01$; (***) $P < 0.001$. (*B*) A 5% red oil staining of frozen liver sections from sham or OVX mice treated for 1 mo, as indicated. In each case, the *Lower* is an enlargement of the region located within the square as indicated in the *Upper*. (*C*) Q-RT-PCR for transcripts of FASN and SCD1 genes in livers of sham or OVX mice treated for 1 mo as indicated. The data correspond to the mean ± SEM for, at least, four mice per treatment. The statistical significance was calculated by Student *t* test; (*) $P < 0.05$; (**) $P < 0.01$. (*D*) Luc assays of Cos-1 cells transfected with pGL3-17mer-estrogen response element (ERE) reporter and pSG5-ER. Cells were treated with Dex, estradiol, CpdX, or CpdX-D3 (0.5 μM) with or without tamoxifen (5 μM) for 6 h. The data correspond to the mean ± SEM for, at least, three independent transfection experiments. The statistical significance was calculated by Student *t* test; (***) $P < 0.001$; (ns): not significant. (*E*) Luc assays of Cos-1 cells transfected with pLuc-TK-2xPRE reporter and pSG5-PR. Cells were treated with Dex, progesterone, CpdX, or CpdX-D3 (0.5 μM) for 6 h. The data correspond to the mean ± SEM for, at least, three independent transfection experiments. The statistical significance was calculated by Student *t* test; (***) $P < 0.001$; (ns): not significant.

activity could be induced selectively by estradiol but not by Dex, CpdX, or CpdX-D3 (Fig. 6*D*). Taken altogether, these results clearly demonstrate that CpdX and CpdX-D3 are devoid of estrogenic and progesterone activities.

Discussion

CpdX, CpdX-D3, and Their Enantiomers Are Bona Fide SEGRAMs. In our accompanying report (16), we demonstrated that CpdX, its deuterated form CpdX-D3, as well as their respective enantiomers are as efficient as synthetic GCs (e.g., Dex) at repressing inflammations generated in several mouse disease models. Importantly, we have now demonstrated that these CpdX compounds are bona fide SEGRAMs as none of the well-known GC-associated debilitating effects have been observed upon their long-term administration (up to 3 mo). Indeed, a daily topical treatment of mouse dorsal skin with CpdX, CpdX-D3, or any of their enantiomers did not induce an epidermal skin atrophy (Fig. 1) nor did a 3-mo daily s.c. injection of these compounds affect the formation of cortical and trabecular bones (Fig. 2 *A–E*) induce a growth inhibition (Fig. 3*A*), changes in body composition (Fig. 3 *B* and *C*), or apoptosis of lymphoid organs (thymus and spleen, see Fig. 3 *D* and *E*) (37). Moreover, unlike Dex, CpdX and CpdX-D3 treatments did not result in an adrenal insufficiency (Figs. 3*G* and 4), hyperglycemia (Fig. 5 *A* and *B*), hyperinsulinemia (Figs. 5*C* and 6*A*), an insulin resistance (Fig. 5 *D* and *E*), or a fatty liver (Figs. 5 *F–H* and 6 *B* and *C*).

Several of the Debilitating Side Effects Generated by Administration of Synthetic GCs Are Due to nGRE-Mediated Transrepression and Can Be Prevented by CpdX Administration. We previously pointed out the important role played by IR nGREs in the generation of GC-induced debilitating effects (3). We have now identified several putative IR nGRE binding sites in the promoter region of the kindlin1, Cyp11a, Cyp11b1, and HSD3β genes (Fig. 4*B*), thereby revealing the mechanism through which Dex but not CpdX compounds induces skin atrophy, osteoporosis, and inhibition of corticoids synthesis.

Long-term treatments with a high dose of synthetic GCs (e.g., Dex and prednisolone) are known to induce an adrenal gland atrophy, similar to that occurring in Addison's disease (38). We have shown that a long-term treatment with Dex induces an adrenal insufficiency, whereas a similar treatment with CpdX, CpdX-D3, or any of their enantiomers did not induce an atrophy of the adrenal fasciculata and glomerulosa zones where the corticosterone and the aldosterone are produced, respectively. Indeed, CpdX compounds do not repress the nGRE-mediated expression of the Cyp11a, Cyp11b1, HSD3β, and Cyp11b2 genes that control the corticosterone and aldosterone synthesis pathways (Fig. 4). In addition, administration of CpdX, CpdX-D3, or of any of their enantiomers maintains a high level of blood corticosterone throughout the whole day (Fig. 4*D*).

Taken altogether, the above data indicate that the beneficial anti-inflammatory effects of CpdX compounds, through repression of proinflammatory genes, result from both: (*i*) The direct binding of CpdX or CpdX-D3 to the GR, which selectively activates its tethered indirect transrepression function and (*ii*) a further activation of this indirect transrepression function due to a CpdX- or CpdX-D3-induced increase in the blood corticosterone level, most notably during the circadian rest period when the ACTH level is the lowest (39). Whether this increase could affect the circadian rhythm of the mouse remains to be seen. In this respect, it is worth mentioning that we did not observe any overt abnormal physical behavior of CpdX-treated mice, compared with control mice.

Substituting the Administration of CpdX Compounds to That of Synthetic GCs Prevents the Occurrence of Both Type 2 Diabetes and Fatty Liver. Worldwide, 0.5% of the general population takes GCs for a variety of therapeutic purposes (40). Some 40–65% of these patients exhibit type 2 diabetes syndrome, which includes hyperglycemia, hyperinsulinemia, and insulin resistance (41, 42). Such GC-induced type 2 diabetes, in association with a GC-induced de novo liver lipogenesis due to activation of liver lipogenic enzymes (e.g., FASN and SCD1, see Fig. 5*G*), leads to fatty liver diseases (31, 43). Moreover, menopause is often associated with an increasing occurrence of insulin-resistant type 2 diabetes and fatty liver syndromes (34), and up to 4.6% of postmenopausal women are taking GCs that exacerbate these syndromes (44).

Importantly, we have shown here that, in the mouse, long-term treatments with CpdX compounds do not induce any sign of type 2 diabetes nor of a fatty liver (Fig. 5). We have also reported that, in OVX mice, taken as a model for menopause, an administration of CpdX or CpdX-D3 prevents the occurrence of such diabetic and hepatic syndromes, in marked contrast with a similar treatment with Dex which further increases the blood glucose level and the lipid deposition in the liver (Fig. 6 *A–C*). Taken altogether, our data strongly suggest that postmenopausal women suffering from inflammatory diseases could be treated with CpdX compounds, instead of GCs, to prevent the possible occurrence of both insulin-resistant type 2 diabetes and liver steatosis.

In short, taken altogether, our data indicate that CpdX compounds exhibit in vivo an anti-inflammatory activity which is similar to that of synthetic GCs (e.g., Dex), whereas being devoid of their undesirable debilitating side effects.

Materials and Methods

Mice. C57BL/6 male and BALB/c female mice were purchased from Charles River Laboratories. Bilateral ovariectomy in mice was performed as described in ref. 35. Breeding, maintenance, and experimental manipulation of mice were approved by the animal care and use committee of the IGBMC/ICS.

RNA isolation and Q-PCR analyses were as in ref. 8. Primers used in the paper are listed in *SI Appendix*, Table S1.

Supporting information includes *SI Appendix, SI Materials and Methods* and Table S1.

ACKNOWLEDGMENTS. We thank Dr. Mei Li for helpful discussions. We also thank the staff of the animal and cell culture facilities of the IGBMC for excellent help, Marie-France Champy (ICS/Institut Clinique de la Souris) for blood analyses, and Alexandru Parlog (ICS/Institut Clinique de la Souris) for bone micro-CT analyses. This work was supported by the Association pour la Recherche à l'IGBMC (ARI), the University of Strasbourg Institute for Advanced Studies (USIAS), the CNRS, and the INSERM. G.H. was supported by a long-term ARI fellowship, whereas N.Z. was supported by an ARI PhD student fellowship.

1. A. R. Clark, M. G. Belvisi, Maps and legends: The quest for dissociated ligands of the glucocorticoid receptor. *Pharmacol. Ther.* **134**, 54–67 (2012).
2. S. H. Meijsing *et al.*, DNA binding site sequence directs glucocorticoid receptor structure and activity. *Science* **324**, 407–410 (2009).
3. M. Surjit *et al.*, Widespread negative response elements mediate direct repression by agonist-liganded glucocorticoid receptor. *Cell* **145**, 224–241 (2011).
4. G. Hua, L. Paulen, P. Chambon, GR SUMOylation and formation of an SUMO-SMRT/NCoR1-HDAC3 repressing complex is mandatory for GC-induced IR nGRE-mediated transrepression. *Proc. Natl. Acad. Sci. U.S.A.* **113**, E626–E634 (2016).
5. C. K. Tan, W. Wahli, A trilogy of glucocorticoid receptor actions. *Proc. Natl. Acad. Sci. U.S.A.* **113**, 1115–1117 (2016).
6. D. Ratman *et al.*, How glucocorticoid receptors modulate the activity of other transcription factors: A scope beyond tethering. *Mol. Cell. Endocrinol.* **380**, 41–54 (2013).
7. D. Langlais, C. Couture, A. Balsalobre, J. Drouin, The Stat3/GR interaction code: Predictive value of direct/indirect DNA recruitment for transcription outcome. *Mol. Cell* **47**, 38-49 (2012).
8. G. Hua, K. P. Ganti, P. Chambon, Glucocorticoid-induced tethered transrepression requires SUMOylation of GR and formation of a SUMO-SMRT/NCoR1-HDAC3 repressing complex. *Proc. Natl. Acad. Sci. U.S.A.* **113**, E635–E643 (2016).
9. M. Baiula *et al.*, Mapracorat, a selective glucocorticoid receptor agonist, causes apoptosis of eosinophils infiltrating the conjunctiva in late-phase experimental ocular allergy. *Drug Des. Devel. Ther.* **8**, 745–757 (2014).
10. H. Schäcke *et al.*, Characterization of ZK 245186, a novel, selective glucocorticoid receptor agonist for the topical treatment of inflammatory skin diseases. *Br. J. Pharmacol.* **158**, 1088–1103 (2009).
11. K. De Bosscher *et al.*, A fully dissociated compound of plant origin for inflammatory gene repression. *Proc. Natl. Acad. Sci. U.S.A.* **102**, 15827–15832 (2005).

12. H. Schäcke *et al*., Dissociation of transactivation from transrepression by a selective glucocorticoid receptor agonist leads to separation of therapeutic effects from side effects. *Proc. Natl. Acad. Sci. U.S.A.* **101**, 227–232 (2004).
13. M. J. Coghlan *et al*., A novel antiinflammatory maintains glucocorticoid efficacy with reduced side effects. *Mol. Endocrinol.* **17**, 860–869 (2003).
14. M.-J. C. van Lierop *et al*., Org 214007-0: A novel non-steroidal selective glucocorticoid receptor modulator with full anti-inflammatory properties and improved therapeutic index. *PLoS One* **7**, e48385 (2012).
15. L. Ripa *et al*., Discovery of a novel oral glucocorticoid receptor modulator (AZD9567) with improved side effect profile. *J. Med. Chem.* **61**, 1785–1799 (2018).
16. G. Hua, N. Zein, F. Daubeuf, P. Chambon, Glucocorticoid receptor modulators CpdX and CpdX-D3 exhibit the same in vivo antiinflammatory activities as synthetic glucocorticoids. *Proc. Natl. Acad. Sci. U.S.A.* **116**, 14191–14199.
17. S. Schoepe, H. Schäcke, E. May, K. Asadullah, Glucocorticoid therapy-induced skin atrophy. *Exp. Dermatol.* **15**, 406–420 (2006).
18. S. Ussar *et al*., Loss of Kindlin-1 causes skin atrophy and lethal neonatal intestinal epithelial dysfunction. *PLoS Genet.* **4**, e1000289 (2008).
19. G. Baida *et al*., REDD1 functions at the crossroads between the therapeutic and adverse effects of topical glucocorticoids. *EMBO Mol. Med.* **7**, 42–58 (2015).
20. F. A. Britto *et al*., REDD1 deletion prevents dexamethasone-induced skeletal muscle atrophy. *Am. J. Physiol. Endocrinol. Metab.* **307**, E983–E993 (2014).
21. J.-Z. Zhang *et al*., BOL-303242-X, a novel selective glucocorticoid receptor agonist, with full anti-inflammatory properties in human ocular cells. *Mol. Vis.* **15**, 2606–2616 (2009).
22. E. Canalis, Mechanisms of glucocorticoid-induced osteoporosis. *Curr. Opin. Rheumatol.* **15**, 454–457 (2003).
23. L. Grahnemo *et al*., Possible role of lymphocytes in glucocorticoid-induced increase in trabecular bone mineral density. *J. Endocrinol.* **224**, 97–108 (2015).
24. H.-F. Zheng *et al*., WNT16 influences bone mineral density, cortical bone thickness, bone strength, and osteoporotic fracture risk. *PLoS Genet.* **8**, e1002745 (2012).
25. M.-F. Champy *et al*., Genetic background determines metabolic phenotypes in the mouse. *Mamm. Genome* **19**, 318–331 (2008).
26. J. J. Cohen, Glucocorticoid-induced apoptosis in the thymus. *Semin. Immunol.* **4**, 363–369 (1992).
27. E. Boucher, P. R. Provost, Y. Tremblay, Ontogeny of adrenal-like glucocorticoid synthesis pathway and of 20α-hydroxysteroid dehydrogenase in the mouse lung. *BMC Res. Notes* **7**, 119 (2014).
28. J. N. Clore, L. Thurby-Hay, Glucocorticoid-induced hyperglycemia. *Endocr. Pract.* **15**, 469–474 (2009).
29. E. B. Geer, J. Islam, C. Buettner, Mechanisms of glucocorticoid-induced insulin resistance: Focus on adipose tissue function and lipid metabolism. *Endocrinol. Metab. Clin. North Am.* **43**, 75–102 (2014).
30. J. Boucher, A. Kleinridders, C. R. Kahn, Insulin receptor signaling in normal and insulin-resistant states. *Cold Spring Harb. Perspect. Biol.* **6**, a009191 (2014).
31. J.-C. Wang, N. E. Gray, T. Kuo, C. A. Harris, Regulation of triglyceride metabolism by glucocorticoid receptor. *Cell Biosci.* **2**, 19 (2012).
32. E. J. Kim *et al*., Cholesterol-induced non-alcoholic fatty liver disease and atherosclerosis aggravated by systemic inflammation. *PLoS One* **9**, e97841 (2014).
33. M. M. Aranha *et al*., Bile acid levels are increased in the liver of patients with steatohepatitis. *Eur. J. Gastroenterol. Hepatol.* **20**, 519–525 (2008).
34. J. Abildgaard *et al*., Ectopic lipid deposition is associated with insulin resistance in postmenopausal women. *J. Clin. Endocrinol. Metab.* **103**, 3394–3404 (2018).
35. M. A. Quinn, X. Xu, M. Ronfani, J. A. Cidlowski, Estrogen deficiency promotes hepatic steatosis via a glucocorticoid receptor-dependent mechanism in mice. *Cell Rep.* **22**, 2690–2701 (2018).
36. M. Lehmann *et al*., Nonsteroidal gestagens (2002). https://patents.google.com/patent/US6344454/en. Accessed 27 March 2019.
37. R. G. Goya *et al*., Glucocorticoid-induced apoptosis in lymphoid organs is associated with a delayed increase in circulating deoxyribonucleic acid. *Apoptosis* **8**, 171–177 (2003).
38. A. Barthel *et al*., An update on Addison's disease. *Exp. Clin. Endocrinol. Diabetes* **127**, 165–175 (2018).
39. A. Mukherji, A. Kobiita, T. Ye, P. Chambon, Homeostasis in intestinal epithelium is orchestrated by the circadian clock and microbiota cues transduced by TLRs. *Cell* **153**, 812–827 (2013).
40. M. C. van der Goes, J. W. Jacobs, J. W. Bijlsma, The value of glucocorticoid co-therapy in different rheumatic diseases–Positive and adverse effects. *Arthritis Res. Ther.* **16** (suppl. 2), S2 (2014).
41. J. L. Hwang, R. E. Weiss, Steroid-induced diabetes: A clinical and molecular approach to understanding and treatment. *Diabetes Metab. Res. Rev.* **30**, 96–102 (2014).
42. A. C. Donihi, D. Raval, M. Saul, M. T. Korytkowski, M. A. DeVita, Prevalence and predictors of corticosteroid-related hyperglycemia in hospitalized patients. *Endocr. Pract.* **12**, 358–362 (2006).
43. J. M. Kneeman, J. Misdraji, K. E. Corey, Secondary causes of nonalcoholic fatty liver disease. *Therap. Adv. Gastroenterol.* **5**, 199–207 (2012).
44. S. Lekamwasam *et al*.; Joint IOF-ECTS GIO Guidelines Working Group, A framework for the development of guidelines for the management of glucocorticoid-induced osteoporosis. *Osteoporos. Int.* **23**, 2257–2276 (2012).